Prediction of Ultrasound-Mediated Disruption of Cell Membranes Using Machine Learning Techniques and Statistical Analysis of Acoustic Spectra

Eva K. Lee*, Richard J. Gallagher, Ann Melissa Campbell, and Mark R. Prausnitz

***Abstract*—Although biological effects of ultrasound must be avoided for safe diagnostic applications, ultrasound's ability to disrupt cell membranes has attracted interest as a method to facilitate drug and gene delivery. This paper seeks to develop "prediction rules" for predicting the degree of cell membrane disruption based on specified ultrasound parameters and measured acoustic signals. Three techniques for generating prediction rules (regression analysis, classification trees and discriminant analysis) are applied to data obtained from a sequence of experiments on bovine red blood cells. For each experiment, the data consist of four ultrasound parameters, acoustic measurements at 400 frequencies, and a measure of cell membrane disruption. To avoid over-training, various combinations of the 404 predictor variables are used when applying the rule generation methods. The results indicate that the variable combination consisting of ultrasound exposure time and acoustic signals measured at the driving frequency and its higher harmonics yields the best rule for all three rule generation methods. The methods used for deriving the prediction rules are broadly applicable, and could be used to develop prediciton rules in other scenarios involving different cell types or tissues. These rules and the methods used to derive them could be used for real-time feedback about ultrasound's biological effects.**

***Index Terms*—Discriminant analysis, drug delivery, machine learning, prediction, ultrasound-mediated cell disruption.**

I. Introduction

RECENT studies suggest that ultrasound is a promising method to control and enhance drug delivery. For example, ultrasound has been shown to transiently disrupt cell membranes, thereby enabling exogenous materials to enter cells without damaging them [1]–[3]. This could facilitate gene therapy by delivering DNA at useful levels to targeted cells. Other studies have demonstrated that ultrasound can dramatically increase skin permeability to a range of compounds, including macromolecules [4], [5]. This could be important for applications such as needle-free delivery of drugs such as insulin. These applications are in marked contrast to traditional diagnostic uses of ultrasound, for which ultrasonic bioeffects are avoided [6].

One of the critical limitations of ultrasound-mediated drug delivery is that ultrasound's effects are difficult to control. Indeed, identical acoustic conditions may have no biological effects, may have reversible effects or may kill cells, depending on the details of the physical environment present during sonication [7]–[9]. It is, therefore, highly desirable to identify conditions that reproducibly cause the intended effects, e.g., reversible membrane disruption for drug delivery applications or no biological effects for diagnostic uses. We propose that such conditions are linked to information contained in the acoustic spectra generated during ultrasound exposure.

Both cell membrane disruption and acoustic spectra are governed by ultrasound-induced cavitation. Cavitation is the creation and oscillation of small gas bubbles that can violently implode if sufficient ultrasound pressures are applied [7], [10]. A number of studies have shown that increased permeability of both skin and cell membranes is caused by a mechanism involving cavitation [9], [11]–[13]. Cavitation occurs as a highly nonlinear and stochastic phenomenon, and ultrasound conditions that cause cavitation are time-dependent and sensitive to the physical environment. Because of this, we believe it is extremely difficult to define ultrasound conditions that will reproducibly disrupt membranes. As an alternative, we propose that one should focus on identifying cavitation conditions that are indicative of membrane disruption. Different ultrasound conditions may be required at different times and in different physical environments to create the same "right" cavitation conditions.

Information about cavitation is present in acoustic spectra. Although details of the relationship between an acoustic spectrum and the associated cavitation field are not known, it is our hypothesis that the cavitation field can be characterized by the acoustic spectrum it emits. Therefore, features of the acoustic spectrum should correlate with cavitation-induced effects on membrane disruption.

This hypothesis has been validated in part by Liu *et al.*, [12] who showed that the degree to which bovine red blood cells were disrupted by ultrasound applied at $f = 24$ kHz over a broad range of ultrasound conditions correlated well with the product of the pressure at half the applied frequency $(P_{f/2})$ and the total duration of ultrasound exposure (τ). This can be regarded as a qualitative measure of the strength of cavitation multiplied by the time over which it acted.

Manuscript received July 3, 2002; revised May 1, 2003. This work was supported in part by grants from the National Science Foundation, and the National Institutes of Health. *Asterisk indicates corresponding author.*

*E. K. Lee is with the Department of Radiation Oncology, Emory University School of Medicine, Atlanta, GA 30322 USA and also with the School of Industrial and Systems Engineering, Georgia Institute of Technology, Atlanta, GA 30332-0205 USA (e-mail: eva.lee@isye.gatech.edu).

R. J. Gallagher is with the Department of Radiation Oncology, Emory University School of Medicine, Atlanta, GA 30322 USA.

A. M. Campbell is with the School of Industrial and Systems Engineering, Georgia Institute of Technology, Atlanta, GA 30332-0205 USA.

M. R. Prausnitz is with the School of Chemical and Biomolecular Engineering and School of Biomedical Engineering, Georgia Institute of Technology, Atlanta, GA 30332-0100 USA.

Digital Object Identifier 10.1109/TBME.2003.820323

Although this single measure may be useful, we sought to utilize a broader representation of the acoustic spectrum to uncover additional correlations which, in combination, could be used to derive robust rules to guide drug delivery applications. With such rules, an intelligent ultrasound device could apply ultrasound to a tissue, "listen" to the acoustic spectrum generated, and use this real-time feedback of information to modify subsequent ultrasound exposure.

In this paper, we describe the application of three machine learning and statistical approaches to derive correlations or "rules" which can predict ultrasound-mediated disruption of red blood cells. By applying these methods to the same data in a like manner, one can see the consistencies and inconsistencies among the methods. This in turn helps to better determine those variables that are most important in predicting membrane disruption. Although the rules generated for red blood cells in this study may not directly apply to other cell types or tissues, we propose that the approach used here may be applied broadly.

Details regarding the methodologies of regression, classification trees and machine learning techniques used in our study are presented in Section II. Empirical tests and analysis of these techniques applied to the acoustic parameters obtained in laboratory experiments on bovine red blood cells are summarized in Section III. Cross-validation techniques are used for an unbiased evaluation of the reliability of the developed rules for future prediction.

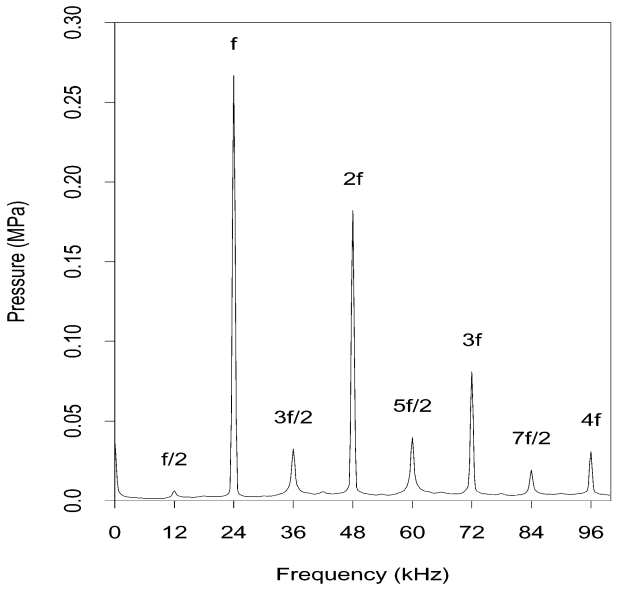

Fig. 1. Measured acoustic spectrum from a representative experiment where ultrasound is applied at 24 kHz (f) with peak incident pressure = 0.902 MPa, total exposure time = 10 s, pulse length = 0.1 s, and duty cycle = 10%. The spectrum is an average collected over the full duration of sonication. Peaks corresponding to harmonics of the driving frequency are often associated with cavitation and are labeled on the graph (e.g., $f/2$, $2f$). The associated degree of cell membrane disruption for this experiment is 73%. Data are from [12].

II. Methods

A. Experimental Data

To develop and validate prediction rules, we used experimental data collected by Liu *et al.* [12]. In their experiments, ultrasound was applied to a suspension of bovine red blood cells at a frequency of 24 kHz using a specified peak incident pressure (0.045–0.902 MPa), pulse length (0.0001–10 s), duty cycle (1%–100%), and total exposure time (0.1–10 s). The ultrasound exposure chamber consisted of a cylindrical piezoelectric transducer measuring 4.5 cm in inner diameter and 2.5 cm in length sandwiched between two 10-cm lengths of PVC pipe. The chamber was filled with filtered, deionized and degassed water. The transducer was controlled by a function generator, whose output was fed to an amplifier and matching transformer to drive the transducer.

Red blood cells were prepared by washing and resuspending at a concentration of 10% by volume in phosphate-buffered saline prepared using gassy, de-ionized water. Red blood cell samples were placed in sample tubes by cutting a 15 ml polypropylene centrifuge tube at the 4-ml line and sealing the top with a rubber stopper, taking care to prevent entrapment of macroscopic air bubbles. Sonication was carried out at room temperature ($22 \pm 2\,^{\circ}\mathrm{C}$). During sonication, exposure chambers did not need to be rotated [14] because the extensive cavitation generated at the low frequency and high pressures used in that study caused vigorous mixing within the exposure chamber. During the experiment, a hydrophone and spectrum analyzer were used to measure the amplitude of emitted acoustic signals at frequencies ranging from 0 to 100 kHz. Over the range of frequencies studied, the hydrophone had a flat response. Acoustic spectra were obtained by averaging acoustic signals collected over the full duration of each ultrasound exposure. Additional information about the experimental apparatus and methods can be found in the paper by Liu *et al.* [12]. Fig. 1 shows a representative acoustic spectrum collected during an ultrasound exposure. These ultrasound parameters and acoustic signals are used as the inputs for generating the prediction rules developed in the present study. After ultrasound exposure, the degree of cell membrane disruption was determined by measuring the background-corrected percentage of hemoglobin released from the red blood cells using a new calibration curve generated for each set of experiments. This measure of membrane disruption is the desired output from the prediction rules. It is referred to in the remainder of the paper as the *percentage of disruption*. This experimental protocol was repeated 180 times using various peak incident pressure, pulse length, duty cycle, and total exposure time parameter combinations.

In these experiments we have used red blood cell lysis as a measure of cell membrane disruption caused by acoustic cavitation. The exact conditions that cause disruption of membranes in different types of cells are likely to be different. However, we propose that red blood cell lysis is an indicator of cell membrane disruption that can be used as a model to demonstrate the ability of machine learning techniques and statistical analysis to determine correlations between acoustic spectra and biological effects of ultrasound.

For each of the 180 experiments, the data consist of 400 distinct acoustic measurements (amplitude measured at frequencies of 0–99 750 Hz in increments of 250 Hz), four ultrasound parameters (peak incident pressure, pulse length, duty cycle, and total exposure time), and a measure of membrane disruption. Hence, there are 180 data points, each involving 404 predictor

variables for determining membrane disruption. If one attempts to apply a method such as regression analysis, classification trees, or discriminant analysis to a situation in which there are fewer data points than predictor variables, there are an infinite number of ways one can fit the data points to the model, and no single fit will stand out as being best. Moreover, the prediction rule associated with some arbitrarily selected fit will invariably be inaccurate in classifying new data points. With this in mind, we selected various combinations of predictor variables, each combination ranging in number from 2 to 20, and developed prediction rules based on these combinations. In this way, the number of data points was much greater than the number of predictor variables, thus enabling robust predictions. The selections included not only the major peaks of the acoustic spectra, but also smaller peaks and, in some cases, broad band noise levels as well.

Specifically, visual inspection of the acoustic spectra showed peaks at the applied frequency, f, and higher harmonics (e.g., $2f$); smaller peaks at half the applied frequency, $f/2$, and its higher harmonics (e.g., $3f/2$); and in some cases, elevated broad-band signals between peaks (Fig. 1). These acoustic features are known to be associated with cavitation, [7], [10] and were, therefore, hypothesized to be promising candidates as feature attributes when applying techniques to derive prediction rules [11], [21]. Since the number of broad-band signals measured was very large, and since no single broad-band signal stood out as being particularly distinguishing, rather than selecting individual broad-band signals as attributes (which may be apparatus dependent), averages of signals between peaks were utilized. Specifically, with peaks occurring at multiples of $f/2 = 12$ kHz, we computed eight averages for each experiment: average of signals measured between 2 and 10 kHz, between 14 and 22 kHz, between 26 and 34 kHz, between 38 and 46 kHz, between 50 and 58 kHz, between 62 and 70 kHz, between 74 and 82 kHz, and between 86 and 94 kHz. These broadband noise averages are referred to throughout the paper as $\mathcal{B}_1, \mathcal{B}_2, \ldots, \mathcal{B}_8$, respectively. In summary, the following potentially significant attributes (ultrasound parameters and acoustic features) were considered:

- total exposure time (τ), duty cycle ($\mathcal{D}$), pulse length ($\mathcal{L}$), peak incident pressure ($\mathcal{P}$);
- pressures measured at integral multiples of the driving frequency: $f, 2f, 3f, 4f$ (collectively referred to throughout the paper as kf);
- pressures measured at odd integer multiples of half the driving frequency: $f/2$, $3f/2$, $5f/2$, $7f/2$ (collectively referred to as $(2k-1)f/2$);
- averages of pressures corresponding to broad band noise between peaks: $\mathcal{B}_1, \ldots, \mathcal{B}_8$ (collectively referred to as $\mathcal{B}$).

Although experimental measurements of membrane disruption are provided on a continuum basis (i.e., 0%–100%), [12] for our study we categorized the data into three discrete groups: 0%–3%, 3%–30%, and 30%–100% membrane disruption. The first group was selected to represent little or no effect; the middle group represents a moderate, and perhaps desired, effect; and the third group represents a strong, and perhaps undesirable, effect. These cutoff points of 3% and 30% were selected to serve as examples. Different cell types and different applications will likely require different cutoff points and possibly different numbers of groups. However, the methods presented in this paper are general and should be applicable to other scenarios.

We chose this approach of discrete classification for two reasons. First, it is unlikely that the feedback provided to a clinician or ultrasound device needs to contain the exact level of membrane disruption. This feedback should often be sufficient if it identifies ultrasound's effects as within a target range, too high or too low. Second, many machine learning techniques do not provide continuum predictions, but classify data into one of a discrete set of groups.

B. Tenfold Cross-Validation

As described below, the data analysis software package S-Plus version 5 (MathSoft; Seattle, Washington) was used to conduct both the regression and classification tree analysis. Linear discriminant analysis was performed using the method described in Lee *et al.* [15]. To obtain an unbiased estimate of the reliability and quality of the derived classification rules, tenfold cross-validation was performed. In the tenfold cross-validation procedure, a dataset is randomly partitioned into ten subsets of equal size. Ten trials are then run, each of which involves a distinct training set made up of nine of the ten subsets and a test set made up of the remaining subset. The classification rule obtained via a given training set is applied to each point in the associated test set to determine to which group the rule allocates it. In our case, there are 180 data points; so in each trial, 162 points are used as the training set to derive a classification rule, and 18 points are used as the test set to gauge the accuracy of the derived rule. As one rotates through the ten trials, each of the 180 points is held back exactly once for use in a test set. In Section III-A we report results in terms of the percentage of test set points correctly classified over the ten trials.

C. Regression Analysis

Regression analysis is generally well-known (e.g., [16] and [17]). We used the S-Plus function lm to fit both first-order (i.e., linear) and second-order models to the training data. To classify test set data points, the predicted percentage of disruption was first calculated based on the fitted regression equation. Depending on this predicted value (less than 3%, between 3% and 30%, greater than 30%), the data point was assigned to one of the three groups. Thus, even though regression analysis yielded continuum predictions, we converted those predictions into discrete classifications to facilitate comparison with the other two prediction rules developed.

D. Classification Trees

Classification trees are used to predict membership of cases or objects in the classes of a categorical dependent variable from their measurements on one or more predictor variables. A classification tree is derived from a training sample via a method known as *recursive partitioning*, whereby the data are successively split along coordinate axes of the predictor variables so that at any node, the split which maximally distinguishes the response variable in the left and the right branches is selected (e.g.,

TABLE I
COMBINATIONS OF ATTRIBUTES USED TO PREDICT RED BLOOD CELL DISRUPTION

Attribute Combination	Exposure Time, τ	Peak Incident Pressure, $\mathcal{P}$	Pulse Length, $\mathcal{L}$	Duty Cycle, $\mathcal{D}$	Pressure[1] at $f/2$	f	$2f$	kf $k=1,2,3,4$	$(2k-1)f/2$ $k=1,2,3,4$	$\mathcal{B}_j$ $j=1,\ldots,8$
1	×	×	×	×						
2	×				×					
3	×					×				
4	×						×			
5	×				×	×				
6	×	×	×	×				×		
7	×	×	×	×					×	
8	×	×	×	×				×	×	
9	×	×	×	×						×
10	×	×	×	×				×	×	×
11	×							×		
12	×								×	
13	×							×		×
14	×								×	×
15	×							×	×	

[1] $kf,\ k=1,2,3,4$, represents the four distinct attributes $f,\ 2f,\ 3f,\ 4f$ used simultaneously.
$(2k-1)f/2,\ k=1,2,3,4$, represents the four distinct attributes $f/2,\ 3f/2,\ 5f/2,\ 7f/2$ used simultaneously.
$\mathcal{B}_j,\ j=1,\ldots,8$, represents the eight averages corresponding to the broadband noise ranges specified in the text, used simultaneously.

see [18]). Splitting continues until nodes are pure or data are too sparse. Terminal nodes are called leaves, and the initial node is called the root. Compared with linear and additive models, tree-based models tend to be more adept at capturing nonadditive behavior and allowing more general (i.e., other than that of a particular multiplicative form) interactions between predictor variables. We used the S-Plus function *tree* to grow a classification tree from training data.

E. Discriminant Analysis via Linear Programming

Like classification trees, discriminant analysis is used to predict membership in the classes of a categorical variable. It is an area that has been extensively researched, and many methods exist for deriving discriminant rules (i.e., classification rules) (e.g., see [19]). The method used herein involves an optimization model developed by Lee *et al.* [15], [20] based on linear programming which associates a penalty with each misclassified training set entity. Linear constraints are utilized to partition the space of predictor variables into polygonal regions representing the classes. Each penalty is scaled according to the associated entity's distance from the region where it belongs. The optimization objective is to minimize the sum of all such penalties. The prediction rule resulting from this model is represented by a set of linear functions, one function for each class, whose variables are a nonlinear transformation of the predictor variables. If L_h denotes the linear function associated with class h, and if y denotes the transformed vector of predictor variables for an entity, then the entity is classified into group g if $L_g(y) \geq L_h(y)$ for $h \neq g$.

III. COMPUTATIONAL EXPERIMENTS AND EMPIRICAL RESULTS

A. Comparison of Prediction Rules

In applying the three methods for generating prediction rules (regression, linear discriminant analysis, classification trees), variables representing some combination of the selected attributes (τ, $\mathcal{D}$, $\mathcal{L}$, $\mathcal{P}$, kf, $(2k-1)f/2$, $\mathcal{B}$) were used. Extensive numerical tests using these methods were conducted to test the effectiveness of approximately 50 combinations of the selected attributes. Combinations which yielded correct cross-validation prediction rates of less than 60% were deemed unacceptable, and are not presented herein. Table I summarizes the attribute combinations for which correct prediction rates exceeded 60%.

For each attribute combination in Table I, each of the three classification methods was applied using the tenfold cross-validation procedure. Fig. 2 shows the percentage of test points correctly classified over the ten trials. To aid in analyzing the results, the attribute combinations are ordered from best to worst according to the resulting scores from the discriminant analysis method (DALP). Note that the same attribute combination (τ, kf) yielded the best rule for all three methods (77.8% for regression, 75.6% for tree classification and 78.9% for DALP). The numerical rules derived from each method for this combination are given in Section III-C. The fact that all three methods performed best with this combination suggests that it is indeed an important combination to consider when developing prediction rules for ultrasound-induced membrane disruption.

We also note that Fig. 2 indicates that alternative attribute combinations involving τ and kf—plus additional attributes—yield percentage scores close to those achieved when using (τ, kf) alone. While the additional attributes do not significantly diminish the predictive ability of the resulting rule, neither do they strengthen it. This observation adds weight to the conclusion that τ and kf hold significant power for predictive capability.

It is interesting to note that, for the regression analysis approach, the attribute combination τ, $\mathcal{P}$, $\mathcal{L}$, $\mathcal{D}$, $\mathcal{B}$, involving the four ultrasound parameters and the broad band noise averages yields a prediction rule that performs equally well as the regression rule derived from τ, kf (both are 77.8% accurate). However, the former combination results in less favorable outcomes for tree classification and discriminant analysis, suggesting that it may not be as reliable a combination for generating prediction rules. A similar observation can be made for the attribute combination $\tau, 2f$. However, in this case, not only did the regression rule perform as well as the rule derived from τ, kf, but the rule generated from the classification tree approach was the second best tree rule, with an accuracy of 74.4% (versus 75.6% for the best tree rule). This suggests that exposure time and the second harmonic alone hold significant predictive power.

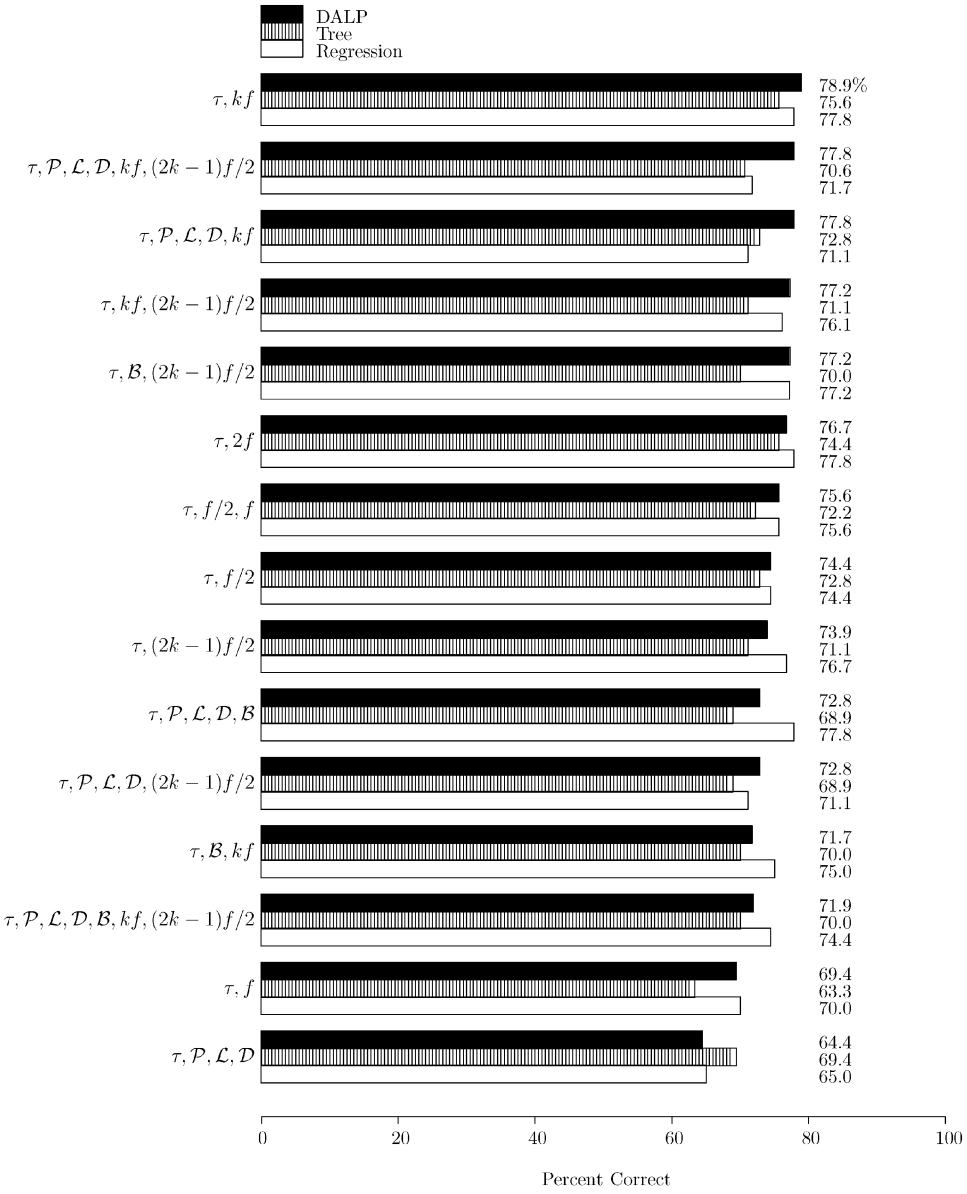

Fig. 2. Summary of tenfold cross-validation experiments showing percentage of test points correctly classified for each method applied to each attribute combination. The combination consisting of τ, kf yielded the best predictive ability according to all three methods.

The achieved accuracy from any prediction rule method is highly dependent on the data to which it is applied. For example, among 24 data sets in the University of California at Irvine Machine Learning Database Repository, achieved accuracies range from 55% to 100% [22]. (The UCI Repository is a collection of data sets from various application areas used by researchers working in the area of machine learning to test new methodologies.) Low accuracy rates are indicative that the data do not provide enough information to easily discriminate among the groups, while high accuracy rates are indicative that the groups are well-separated based on the data. Given the mixed data set considered herein, the maximum achieved accuracy of 78.9% is promising. (A widely-used test for cervical cancer has a 20% false negative rate [23].) It should be remarked that the selection of attributes to include in a model is a difficult problem. While our empirical results indicate that the attribute combinations selected for this study are good choices, we do not rule out the possibility that other combinations may ultimately provide more accurate prediction rules.

B. Implications of Prediction Rules

All but one of the 15 attribute combinations which yielded reasonable predictions (i.e., $>$60% accuracy) require information from the acoustic spectrum (e.g., kf, $(2k-1)f/2$, $\mathcal{B}$), indicating that acoustic signals provide valuable information about ultrasound's effects. The attribute combination that includes only information about applied ultrasound parameters (i.e., τ, $\mathcal{P}$, $\mathcal{L}$, $\mathcal{D}$) was clearly inferior. This indicates that predicting ultrasound's effects on the basis of applied ultrasound settings, as is typically done, should yield significantly worse predictions than those which use information from the acoustic spectrum.

Many of the attribute combinations contain $(2k-1)f/2$, which are generally associated with inertial cavitation [11], [24]

Some also contain the broadband noise averages $\mathcal{B}$, which are usually associated with transient cavitation [25], [26] This is expected, since membrane disruption by ultrasound is thought to be mediated by cavitation. This is also consistent with earlier, less sophisticated analysis of this dataset, which yielded a correlation between membrane disruption and $f/2$. [12] In addition, all 15 of the attribute combinations in Fig. 2 contain total exposure time (τ), indicating that the duration of exposure to ultrasound (and cavitation) correlates strongly with membrane disruption. This dependence on exposure time may reflect the kinetics of bubble nucleation and growth [27] or may be a feature of the bubble-cell interaction.

It is surprising to note that the best attribute combination does not contain $(2k-1)f/2$ or $\mathcal{B}$. Instead it is based on the total exposure time and the height of the driving frequency peak and its integer harmonics (kf). The height of these peaks is thought to be a measure of the applied ultrasound pressure coupled with resonance characteristics of the experimental device and some features of cavitation. [7], [10] Mechanistically, it is not clear why this attribute combination should provide the best prediction.

From a practical standpoint, the type of prediction rules developed here might be used to guide medical or laboratory application of ultrasound to deliver drugs or genes into cells. We have shown that predictions which use applied ultrasound parameters as well as acoustic spectrum measurements are consistently better than those which rely on applied ultrasound parameters alone. A limitation of these rules may be their absolute prediction accuracy (i.e., $\leq$78.9% accurate), which may not be sufficient to guarantee safety and efficacy for medical protocols. However, the absolute levels of accuracy are not the emphasis of this paper. Rather, comparing the relative levels of accuracy for different predictions demonstrates which attribute combinations and methods hold greatest promise to predict biological effects of ultrasound. Better accuracy may be achieved in future studies.

Another limitation of these rules is that they may not be applicable to other cell types and especially to cells within tissues. Thus, rules that predict red blood cell disruption may not be the same ones that predict effects on other cell types. Cells within tissues may respond to ultrasound differently as well, due to limited intercellular space, low dissolved gas content and increased acoustic absorption, each of which reduce cavitation activity [28]. However, it is this effect of different physical environments on cavitation that in part motivated our approach to developing predictive rules. A given set of ultrasound conditions applied to cells in suspension *in vitro* will generate cavitation that results in certain bioeffects. The same set of ultrasound conditions applied to cells in a tissue *in vivo* will likely generate a different (i.e., lesser) amount of cavitation that will result in different bioeffects. It is our hypothesis that rather than keeping ultrasound exposure constant when moving from *in vitro* cell suspensions to *in vivo* tissues, one should keep the amount of cavitation generated constant, which may require using different and time-varying ultrasound conditions. For this reason, the rules we generated have included measures of cavitation from the acoustic spectrum. Consistent with our hypothesis, rules with information from the acoustic spectrum are more robust than those based solely on ultrasound parameters and may be better suited for *in vitro–in vivo* correlation. Additional studies are needed to validate this hypothesis.

C. Best Prediction Rules

For each classification method, the best rule (as measured by the number of test set entities correctly classified) was that derived using the attribute combination of exposure time, τ, and pressures at kf. Here, we summarize the best prediction rules resulting from each of the three methods.

Regression Analysis: Among the first-order and second-order regression models, the most accurate rule was derived from the first-order model. The associated regression equation is given in (1)

$$\begin{aligned}\mathrm{PredDisrupt} = &-6.3 + 2.0\tau + 6.5\mathrm{P}_f + 193.8\mathrm{P}_{2f} \\ &+50.0\mathrm{P}_{3f} - 171.9\mathrm{P}_{4f}. \end{aligned} \tag{1}$$

Here, $\mathrm{PredDisrupt}$ denotes the predicted percentage of disruption, the total exposure time (τ) has units of seconds, and the pressure terms (P_f, P_{2f}, P_{3f}, and P_{4f}) have units of MPa. Note that the coefficient for P_{2f} is largest in magnitude, suggesting a prominant role for this attribute in terms of predictive power. Although the application of (1) yields an explicit value for $\mathrm{PredDisrupt}$, for this paper we are only interested in predicting disruption to within specified numeric intervals. In particular:

- if $\mathrm{PredDisrupt} < 3.0$, cells are classified into Group 1;
- if $3.0 \leq \mathrm{PredDisrupt} < 30.0$, cells are classified into Group 2;
- if $\mathrm{PredDisrupt} \geq 30.0$, cells are classified into Group 3.

Using the regression equation in this manner allows direct comparison of the regression analysis approach to the classification tree and discriminant analysis approaches below.

Classification Trees: A classification tree is read by traversing the tree from the root node at the top of the tree to a leaf node at the bottom. One follows a path from the root to a leaf according to the splits at nonleaf nodes. If the indicated inequality at a node is satisfied, one follows the left branch; otherwise, one follows the right branch. The tree below was derived from the experimental data, and can be used to classify ultrasound-exposed cells into one of the three disruption categories based on exposure time and measured values of pressures at kf for $k =$ 1, 2, 3, 4.

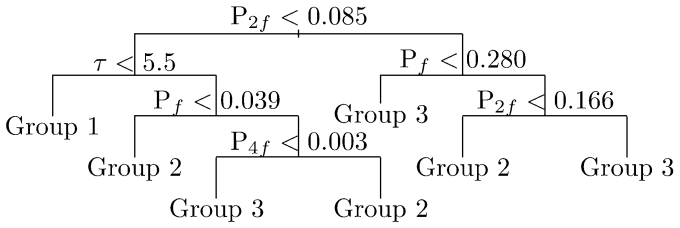

In this tree, pressures (P_{kf}) are expressed in MPa, and exposure time (τ) in seconds. Again, P_{2f} is prominent in terms of predicitve power, as indicated by its role in the split at the top level of the tree.

Discriminant Analysis via Linear Programming: The classification rule derived from the discriminant analysis method is more complicated to state. The first step involves estimating group conditional probability density functions based on the experimental data. For the work presented herein, we used normal model group conditional density estimates assuming a common covariance matrix. That is

$$\hat{f}_g(x) = (2\pi)^{-\frac{k}{2}}|S|^{-\frac{1}{2}} \times \exp\left\{-\frac{1}{2}(x-\bar{x}_g)^T S^{-1}(x-\bar{x}_g)\right\}, \quad g = 1,2,3$$

where $\bar{x}_g$ denotes the sample mean vector for group g, and S denotes the pooled sample covariance matrix (e.g., see [19] or [29]). Based on the experimental data, $\bar{x}_g$ and S are as follows:

$$\bar{x} = \begin{bmatrix} 5.232 \\ 0.069 \\ 0.014 \\ 0.009 \\ 0.007 \end{bmatrix}, \quad \bar{x}_2 = \begin{bmatrix} 9.348 \\ 0.130 \\ 0.042 \\ 0.024 \\ 0.017 \end{bmatrix}, \quad \bar{x}_3 = \begin{bmatrix} 10.000 \\ 0.241 \\ 0.171 \\ 0.092 \\ 0.050 \end{bmatrix}$$

$$S = \begin{bmatrix} 6.895 & -0.065 & -0.024 & -0.015 & -0.009 \\ -0.065 & 0.007 & 0.004 & 0.002 & 0.001 \\ -0.024 & 0.004 & 0.003 & 0.002 & 0.001 \\ -0.015 & 0.002 & 0.002 & 0.001 & 0.001 \\ -0.009 & 0.001 & 0.001 & 0.001 & 0.001 \end{bmatrix}.$$

Here, the first component of $\bar{x}_g$ is the mean of the exposure time of the cells in group g; and the second, third, fourth and fifth components are the means of the pressures measured at kf for $k = 1, 2, 3, 4$ for the cells in group g.

The second step for deriving the discriminant analysis rule involves deriving the linear discriminant functions L_h for $h = 1, 2, 3$. Details for carrying out this step can be found in Lee *et al.* [15]. Here, we simply list the functions derived from the experimental data

$$L_1(x) = \frac{1}{3}\hat{f}_1(x) - 0.00\hat{f}_2(x) - 0.04\hat{f}_3(x)$$
$$L_2(x) = \frac{1}{3}\hat{f}_2(x) - 0.27\hat{f}_1(x) - 0.00\hat{f}_3(x)$$
$$L_3(x) = \frac{1}{3}\hat{f}_3(x) - 0.00\hat{f}_1(x) - 0.00\hat{f}_2(x).$$

In order to use these functions to classify ultrasound-exposed cells, one would form a 5-tuple, say x, with the exposure time, and the measured pressures at kf for $k = 1, 2, 3, 4$, and evaluate the functions L_h at x. If the maximum is $L_1(x)$, then the cells are classified into Group 1 (disruption less than 3%). If the maximum is $L_2(x)$, then the cells are classified into Group 2 (disruption greater than or equal to 3% and less than 30%). If the maximum is $L_3(x)$, then the cells are classified into Group 3 (disruption greater than or equal to 30%).

Classification Matrices for Predictions: Table II shows the classification matrices associated with the three prediction rules presented in this section. For each matrix, the entry in row i, column j records the percentage of group i cells classified into group j. Note that for all three rules, there is a relatively high percentage of group 1 cells mis-classified as group 2. Hence, these methods are not good at distinguishing cell membrane disruption less than the 3% threshold separating groups 1 and 2. In contrast, the accuracy achieved by the regression and the DALP methods for group 3 is in the 90% range, indicating that these methods are quite adept at distinguishing cell membrane disruption above the 30% threshold separating groups 2 and 3. This may be helpful as a means to distinguish between achieving a desired effect (e.g., group 2) and an undesirable one (e.g., group 3). The high rate of misclassification errors for group 1 cells might be due to the narrow membrane disruption range (0%–3%) characterizing this group. In addition, low membrane disruption in this group means that experimental noise or errors in the acoustic measurement contribute to a greater relative error. Rules developed based on different thresholds may prove to be more accurate. Further research is needed to study the sensitivity of generated rules to selected thresholds.

TABLE II
CLASSIFICATION MATRICES ASSOCIATED WITH THE THREE PREDICTION RULES PRESENTED IN SECTION III-C. FOR EACH MATRIX, THE ENTRY IN ROW i, COLUMN j RECORDS THE PERCENTAGE OF GROUP i CELLS CLASSIFIED INTO GROUP j

	Regression				Tree		
	[,1]	[,2]	[,3]		[,1]	[,2]	[,3]
[1,]	51.3	48.7	0.0	[1,]	56.4	38.5	5.1
[2,]	2.6	78.9	18.4	[2,]	2.6	81.6	15.8
[3,]	0.0	7.7	92.3	[3,]	3.1	16.9	80.0

	DALP		
	[,1]	[,2]	[,3]
[1,]	61.5	38.5	0.0
[2,]	6.6	78.9	14.5
[3,]	0.0	10.8	89.2

IV. CONCLUSION

Motivated by the need to control cell disruption caused by ultrasound for drug delivery, we used three independent approaches to determine "rules" that predict the degree of membrane disruption induced by exposure of red blood cells to ultrasound. Cross-validated results from all three approaches—regression analysis, classification trees, and discriminant analysis via linear programming—indicate that the variable combination consisting of total exposure time and acoustic signals measured at integer multiples of the driving frequency yields the best prediction rule for correctly predicting membrane disruption for the cells and conditions examined in this paper.

Rules using applied ultrasound parameters as well as measured attributes of the acoustic spectrum generated during ultrasound exposure yield better predictions than rules based only on applied ultrasound parameters. This demonstrates the value of using measured acoustic signals for predictions. Once a rule is derived, the time required to make a prediction is negligible. Thus, using the approach described here, a robust rule developed for specific types of cells and tissue might be used for real-time feedback control of ultrasound to achieve reproducible cell membrane disruption for drug and gene delivery.

ACKNOWLEDGMENT

The authors would like to thank J. Liu and T. Lewis for helpful discussions.

REFERENCES

[1] M. Fechheimer, J. F. Boylan, S. Parker, J. E. Sisken, G. L. Patel, and S. G. Zimmer, "Transfection of mammalian cells with plasmid DNA by scrape loading and sonication loading," *Proc. Nat. Acad. Sci. USA*, vol. 84, pp. 8463–8467, 1987.

[2] J. A. Wyber, J. Andrews, and A. D'Emanuele, "The use of sonication for the efficient delivery of plasmid DNA into cells," *Pharmaceutical Res.*, vol. 14, no. 6, pp. 750–756, 1997.

[3] D. L. Miller, S. Bao, R. A. Gies, and B. D. Thrall, "Ultrasonic enhancement of gene transfection in murine melanoma tumors," *Ultrasound Med. Biol.*, vol. 25, pp. 1425–1430, 1999.

[4] S. Mitragotri, D. Blankschtein, and R. Langer, "Ultrasound-mediated transdermal protein delivery," *Science*, vol. 269, pp. 850–853, 1995.

[5] E. Camel, "Ultrasound," in *Percutaneous Penetration Enhancers*, E. W. Smith and H. I. Maibach, Eds. Boca Raton, FL: CRC, 1995, pp. 369–382.

[6] S. B. Barnett and G. Kossolf, Eds., *Safety of Diagnostic Ultrasound*. New York: Parthenon, 1998.

[7] T. G. Leighton, *The Acoustic Bubble*. London, U.K.: Academic, 1994.

[8] K. S. Suslick, *Ultrasound: Its Chemical, Physicial and Biological Effects*. Deerfield Beach, FL: VCH, 1988.

[9] M. W. Miller, D. L. Miller, and A. A. Brayman, "A review of *in vitro* bioeffects of inertial ultrasonic cavitation from a mechanistic perspective," *Ultrasound Med. Biol.*, vol. 22, no. 9, pp. 1131–1154, 1996.

[10] S. B. Barnett, "Nonthermal issues: cavitation—its nature, detection and measurement," *Ultrasound Med. Biol.*, vol. 24, pp. S11–S21, 1998.

[11] P. D. Edmonds and P. Ross, "Acoustic emission as a measure of exposure of suspended cells *in vitro*," *Ultrasound Med. Biol.*, vol. 12, pp. 297–305, 1986.

[12] J. Liu, T. N. Lewis, and M. R. Prausnitz, "Non-invasive assessment and control of ultrasound-mediated membrane permeabilization," *Pharmaceutical Res.*, vol. 15, pp. 918–924, 1998.

[13] S. Mitragotri, D. A. Edwards, D. Blankschtein, and R. Langer, "A mechanistic study of ultrasonically-enhanced transdermal drug delivery," *J. Pharmaceutical Sci.*, vol. 84, no. 6, pp. 697–706, 1995.

[14] M. W. Miller, C. C. Church, A. A. Brayman, M. S. Malcuit, and R. W. Boyd, "An explanation for the decrease in cell lysis in a rotating tube with increasing ultrasound intensity," *Ultrasound Med. Biol.*, vol. 15, pp. 67–72, 1989.

[15] E. K. Lee, R. J. Gallagher, and D. A. Patterson, "A linear programming approach to discriminant analysis with a reserved judgment region," *INFORMS. J. Computing*, vol. 15, no. 1, pp. 23–41, 2003.

[16] N. R. Draper and H. Smith, *Applied Regression Analysis*, 2nd ed. New York: Wiley, 1981.

[17] J. Neter, W. Wasserman, and M. H Kutner, *Applied Linear Statistical Models*, 3rd ed. Homewood, IL: Irwin, 1990.

[18] L. Breiman, J. H. Friedman, R. A. Olshen, and C. Stone, *Classification and Regression Trees*. Belmont, CA: Wadsworth, 1984.

[19] G. J. McLachlan, *Discriminant Analysis and Statistical Pattern Recognition*. New York: Wiley, 1992.

[20] R. J. Gallagher, E. K. Lee, and D. A. Patterson, "Constrained discriminant analysis via 0/1 mixed integer programming," *Ann. Operations Res.—Non-Traditional Approaches to Statistical Classification and Regression*, vol. 74, pp. 65–88, 1997.

[21] E. C. Everbach, I. R. S. Makin, M. Azadniv, and R. S. Meltzer, "Correlation of ultrasound-induced hemolysis with cavitation detector output *in vitro*," *Ultrasound Med. Biol.*, vol. 23, pp. 619–624, 1997.

[22] C. L. Blake and C. J. Merz. (1998) UCI Repository of Machine Learning Databases. Univ. California, Dept. Inform. Comput. Sci., Irvine, CA. [Online]. Available: http://www.ics.uci.edu/~mlearn/MLRepository.html

[23] J. Gay, L. Donaldson, and J. Goellner, "False-negative results in cervical cytologic studies," *Acta Cytologica*, vol. 29, pp. 1043–1046, 1985.

[24] E. A. Neppiras, "Subharmonic and other low-frequency emission from bubbles in sound-irradiated liquids," *J. Acoust. Soc. Amer.*, vol. 46, pp. 587–601, 1968.

[25] ——, "Measurement of acoustic cavitation," *IEEE Trans. SU*, vol. 15, pp. 81–88, 1968.

[26] C. K. Holl and R. E. Apfel, "Thresholds for transient cavitation produced by pulsed ultrasound in a controlled nuclei environment," *J. Acoust. Soc. Amer.*, vol. 88, pp. 2059–2069, 1990.

[27] H. G. Flynn and C. Church, "Transient pulsations of small gas bubbles in water," *J. Acoust. Soc. Amer.*, vol. 84, pp. 985–998, 1988.

[28] S. B. Barnett, "Other nonthermal bioeffects: organs, cells and tissues," *Ultrasound Med. Biol.*, vol. 24, pp. S35–S39, 1998.

[29] T. W. Anderson, *An Introduction to Multivariate Statistical Analysis*, 2nd ed. New York: Wiley, 1984.

Eva K. Lee received the Ph.D. degree from the Department of Computational and Applied Mathematics at Rice University, Houston, TX, in 1993.

She holds a joint faculty appointment in the Department of Radiation Oncology at Emory University, Atlanta GA, and the School of Industrial and Systems Engineering at the Georgia Institute of Technology, Atlanta. Her research focuses on mathematical modeling and algorithmic design of biomedical problems, pattern recognition, classification, large-scale optimization and computing, and applications of these technologies to disease/cancer diagnosis and prediction, optimal treatment design, and efficient drug delivery.

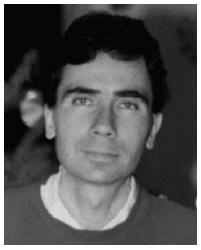

Richard J. Gallagher received the Ph.D. degree in mathematics from the University of Nebraska at Lincoln in 1988. He completed a postdoctoral training program in medical informatics at Columbia University, New York.

He is currently a Senior Programmer Analyst at First Consulting Group Management Services, where he is part of a group responsible for maintaining information security at a large multicentered academic hospital. He holds the honorary title of Adjunct Assistant Professor in the computational research and informatics division of the Department of Radiation Oncology at Emory University, Atlanta, GA.

Ann Melissa Campbell received the undergraduate degree in computational and applied mathematics from Rice University, Houston, TX, in 1993, and the Ph.D. degree in industrial engineering from the Georgia Institute of Technology, Atlanta, in 2000.

She is an Assistant Professor in the Department of Management Sciences in the Tippie College of Business at the University of Iowa, Iowa City. Her current research is focused on using optimization with problems in freight distribution; in particular, vehicle routing and dynamic load pricing.

Mark R. Prausnitz received the B.S. degree from Stanford University, Stanford, CA, in 1988, and the Ph.D. degree from the Massachusetts Institute of Technology, Cambridge, in 1994.

He is Associate Professor of Chemical and Biomedical Engineering at the Georgia Institute of Technology, Atlanta. His research interests concern novel uses of ultrasound, electric fields, and microfabricated devices to enhance and target drug delivery.